Production and Monitoring of Neutron Flux by Activation Detectors

Ivan Haysak[1], Vasyl Martishichkin[1], Yevgen Harapko[1], Robert Holomb[1,2], and Karel Katovsky[2]
[1]Uzhgorod National University, Ukraine
[2]Brno University of Technology, Czech Republic
Corresponding author: ivan.haysak@uzhnu.edu.ua

***Abstract*—The neutron generation technique was tested on the microtron M-10 with an output electron beam of 8.7 MeV. Given the low energy that the microtron can provide to electrons, the bremsstrahlung induced photonuclear reaction ^{9}Be (γ, n), which has a low threshold, was chosen for neutron generation. Cobalt and indium targets were tested as activation detectors to estimate the neutron flux density. In the cobalt target, the isomeric state of ^{60m}Co with an energy of 58.6 keV and a half-life of 10.5 minutes is well activated. Two well-known additional gamma lines of standard cobalt source permit to clarify the absolute value of the neutron flux. The activated indium target has four gamma lines bound to the ^{116m}In isomer β^- decaying with the half-life of 54.4 minutes, what is convenient for measurement of gamma spectrum. Despite the low energy of the output electron beam, at a beam intensity of 5 μA it is possible to obtain an almost isotropic neutron flux of 10^7 n/(s·cm^2).**

***Keywords* — Neutron production, microtron, gamma spectroscopy, neutron activation detectors.**

I. Introduction

On the microtron M-10 of Uzhgorod National University there are carried out experimental investigations of photonuclear reactions [1] as well as applied studies of irradiation influence on the properties of new technological materials and electronical components [2]. For irradiation it is possible to use electrons of energies 4-10 MeV and bremsstrahlung. But it was demonstrated [3] that low energy electron accelerator microtron MT-25 with 22 MeV output electron beam can serve as neutron source, which is interesting to compare with the generation of neutrons by a proton accelerator at the same beam energies [4].

Neutrons are unique particles that are of interest from both a fundamental and an applied point of view. Of the unsolved experimental fundamental problems, we note the problem of neutron lifetime [5], the question of the presence of the electric dipole moment of the neutron [6], and the search for neutron clusters [7]. In addition, neutron registration still represents an uneasy problem.

Among the current applied research, we note the study of different types of structures in the physics of condensed matter, the study of the effect of neutron fluxes on living tissues and organisms, neutron diffraction analysis [8], neutron activation analysis. Of great practical importance for materials science is the availability of accurate data on the cross-sections of the interaction of neutrons with nuclei. For energy needs, namely for reactors controlled by accelerators, experimental data on neutron generation processes are required.

In this paper, we present the results of neutron generation on the M-10 microtron of Uzhgorod National University. The experiment consist of few stages – 1) output electron beam generate bremsstrahlung spectrum in reaction $e^- + Z \rightarrow \gamma + e^- + Z$, 2) neutrons creation in photonuclear reaction (γ,n), 3) activation reaction (n,γ) and 4) measuring and analysis of gamma spectra of activated sample.

II. Experimental set up

A. Schematic view

The Fig. 1 shows a schematic of the experiment. The output electron beam falls on the braking tungsten target after which the bremsstrahlung beam hits the beryllium target. Neutrons are created on a beryllium target in reaction

$$\gamma + {}^{9}Be \rightarrow \mathrm{n} + 2\alpha, \qquad (1)$$

starting from the threshold E_γ=1.57 MeV. The intensity of generated neutrons is registered by the activation sample (target) due to (n, γ) reaction. Analysis of gamma spectra of the activated sample (detector) gives the value of the neutron flux.

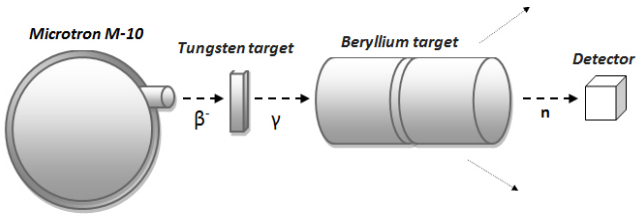

Fig. 1. Schematic of the experiment: accelerator microtron M-10, tungsten gamma converter, the beryllium target and the activation target (detector).

The main parameters of our experiment were as follows: the energy of the induced electron beam was 8.7 MeV and a plate of natural tungsten of size 93 x 55 x 2 mm (thickness 2 mm) served as a braking target. The size of the beryllium target is Ø10 x 14 cm, and its weight is 2 kg.

To measure neutrons flux we use ^{59}Co as activation detectors. The cobalt detector (boxed powder $CoCO_3$*$Co(OH)_2$*nH_2O, mass 31 g) was irradiated during 10 min by neutrons Cobalt

detector is activated by neutrons to both ^{60}Co ground state and isomeric level ^{60m}Co with half-life 10.47 minutes and following isomeric transition E_γ = 58.6 keV to the ground state. After β-decay (half-time 5.27 years) the ground state gives well-known two lines E_γ = 1173 keV and E_γ = 1332 keV [9]. As a neutron indicator, we also used an aluminum plate coated with indium powder.

B. Gamma Spectrometer

A NaI(Tl) crystal scintillation detector with size Ø63 x 63 mm looking through by photomultiplier 19-M and with the SBS-40 amplitude analyzer board served as a gamma spectrometer (Fig. 8). The accumulation of spectra occurs with the help of a specialized computer program AkWin. The number of channels of the analyzer is variable and can take values from 256 to 8192.

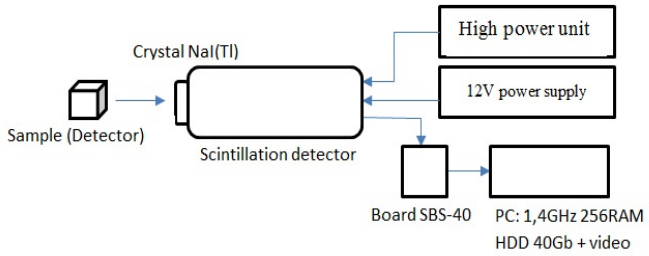

Fig. 2. Schematic of the scintillation spectrometer.

The measured energy resolution (FWHM) of the spectrometer for calibration lines and the simulated total peak efficiency ε for the detected gamma lines of the neutron-activated sample 59Co are shown in Table I.

TABLE I
THE EFFICIENCY AND THE ENERGY RESOLUTION OF THE GAMMA SPECTROMETER

E_γ, keV	58.6	59.5	661.7	1173	1332
ε × 10^2	23.2	-	-	4.71	4.16
FWHM keV	-	16.2(2)	71.2(3)	82.0(5)	88.8(9)

III. BREMSSTRAHLUNG SPECTRUM

The gamma-ray spectrum created on a 2 mm thick tungsten target in the forward direction by a 5 MeV electron beam is showed at the Fig. 2. The spectrum is simulated by the FLUKA code [10]. The bremsstrahlung spectrum is a wide peak in the interval of energy $E\gamma$=0.1-5 MeV. In the energy region, less than 0.1 MeV the characteristic X-ray lines of tungsten atom are present, also the annihilation line of 0.511 MeV is evident. That is, in a tungsten conversion target with a thickness of 2 mm, there is a significant probability of a three-stage process, namely, 1) the braking process on the nucleus $e^- + Z \rightarrow \gamma + e^- + Z$; 2) formation in the field of the nucleus of electron-positron pairs $\gamma + Z \rightarrow e^+ + e^- + Z$; 3) the formation of the positronium atom $e^+ + e^- \rightarrow Ps$; 4) annihilation of positronium $Ps \rightarrow \gamma + \gamma$. The first two processes take place with the participation of the atomic nucleus, and the last two are the atomic processes.

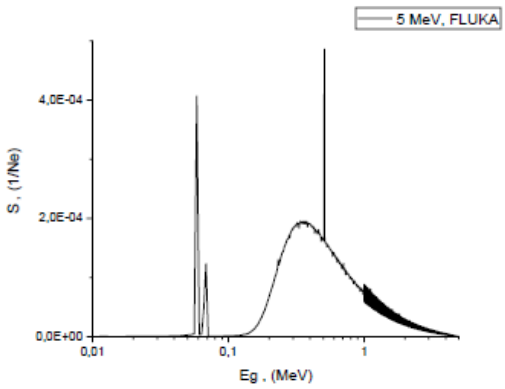

Fig. 3. The simulated braked gamma spectrum of 5 MeV electron beam in 2 mm tungsten converter.

In Fig. 3 is shown a comparison of the bremsstrahlung spectra simulated for electron beam of energies 4 MeV, 5 MeV, 8 MeV, and 9 MeV [11]. It is seen that the shape of the peak is preserved, and with increasing electrons energy the yield of gamma quanta is increased. In the study of nuclear reactions, only a part of the gamma spectrum with energy greater than the reaction threshold "works". In our case of neutrons generation on a beryllium target, it is gamma quanta with energies greater than 1.6 MeV. But at a set of the absorbed dose, it is necessary to consider the whole bremsstrahlung spectrum.

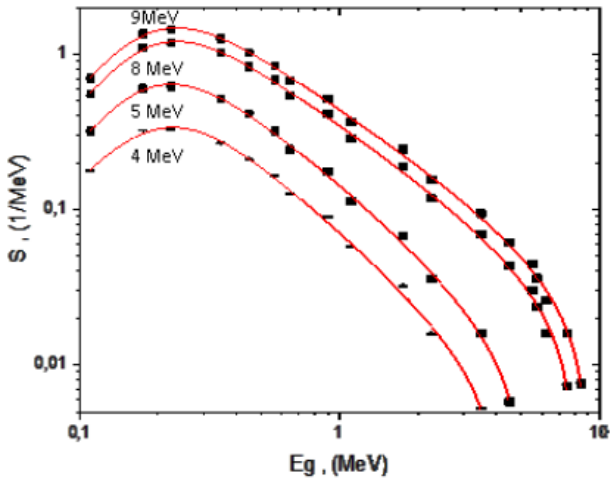

Fig. 4. The simulated bremsstrahlung for different electron beam energies 4, 5, 8 and 9 MeV.

It should be noted that the bremsstrahlung spectrum depends on both the electron energy and the thickness of the braking target and its atomic composition. The penetration depth of a monoenergetic electron beam with energies $3 < E_e < 20$ MeV in aluminum is well described by phenomenological formula

$$R = 0.53 \cdot E_e - 0.106\,, \qquad (2)$$

where R is the depth of penetration in g/cm^2, E_e is the electron energy in MeV [12]. For other matter the penetration depth can be estimate by correction

$$R_x = R_{Al}\frac{(Z/A)_{Al}}{(Z/A)_x}, \quad (3)$$

where $(Z/A)_x$ is the charge to mass ratio of the corresponding element. The estimated penetration depth for an electron beam of 8.7 MeV in tungsten is 2.8 mm.

IV. Neutron Production

The measured and evaluated data of the energy dependence of the photonuclear reaction cross-section *σ(γ, abs)* for beryllium, is as follows Fig. 4. For electron energy of 8.7 MeV(and maximal energy of gamma), the cross-section is about 1.5 mb. Up to threshold energy of channel *(γ, p)* 16.89 MeV there are open channels *(γ,nx)* where *x* are 2α or ^{8}Be

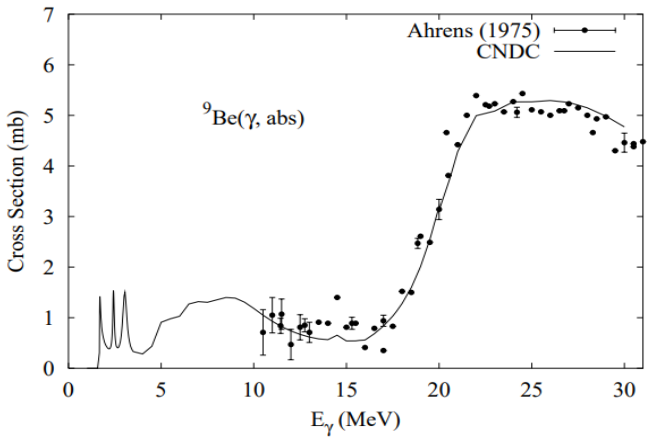

Fig. 5. The measured and the model calculation of the total cross-section of photoabsorption reaction ^{9}Be(γ,abs) [13].

in the ground or excited states (the three lowest well-separated levels of ^{8}Be are 3.04, 11.4, and 16.6 MeV). The thresholds of these channels are indicated in Table I. So for electron beam 8.7 MeV the three channels of reaction ^{9}Be(γ,n) are opened.

TABLE II
THE THRESHOLD ENERGIES FOR DIFFERENT REACTION CHANNELS

Threshold energies (MeV)			
γ, n+2α	γ, n+^{8}Be	γ, n+^{8}Be*(3.04)	γ, n+^{8}Be*(11.4)
1.57	1.67	4.71	13.1

Analysis of the kinematics of the ^{9}Be(γ, n)^{8}Be reaction shows that the kinetic energy of a neutron is weakly dependent on its emission angle. Fig. 5 given the dependence of the neutron kinetic energy distribution versus the angle of the outgoing neutron relative to the gamma beam direction for energies of gamma quanta 8, 6, 4, and 2 MeV. However, the shape of the angular distribution can be deformed by the dynamics (matrix element) of the nuclear reaction. Fig. 3 shows that the intensities of the corresponding energies of gamma quanta differ by an order of magnitude. That is, one can conclude that the reaction (γ, n) forming an almost isotropic distribution of neutrons in the whole energy region from zero up to 6 MeV. But in the beryllium target itself, neutrons are moderated by elastic multiple scattering on beryllium nuclei. Therefore, the spectrum of neutrons outside the beryllium target will be much softer.

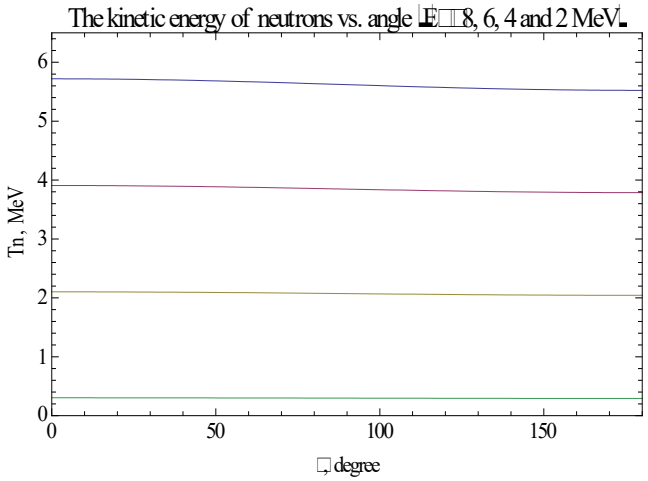

Fig. 6. The angle dependence of kinetic energy of outgoing neutrons for reaction γ + ^{9}Be → n + ^{8}Be at energy E$_γ$=8, 6, 4 and 2 MeV (violet, red, yellow, and green line respectively).

V. Activation Detectors

We chose samples of ^{59}Co and natural indium as activation detectors which have satisfactory rate activation and disintegration constants. The activation sample was located close to the side surface of the beryllium cylinder.

A. Cobalt sample

The effective cross-section of the reaction ^{59}Co(n,γ) is shown in Fig. 6. In the region from thermals up to 6 MeV neutrons, the cross-section belongs to interval 2-40 barns [14].

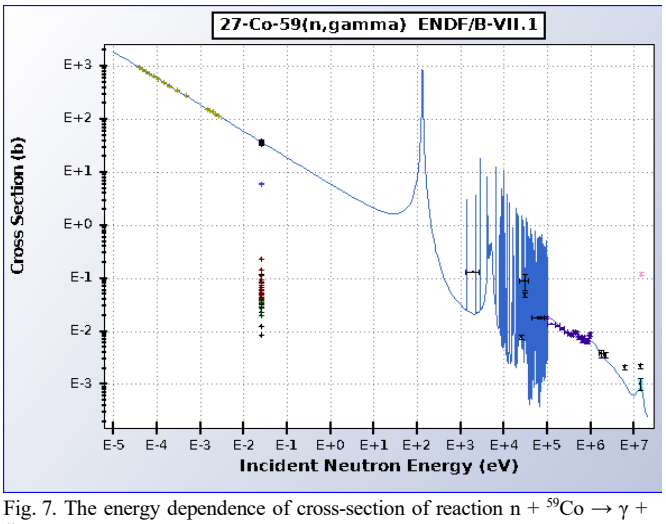

Fig. 7. The energy dependence of cross-section of reaction n + ^{59}Co → γ + ^{60g,m}Co [14].

Neutron activation of ^{59}Co leads to the formation of ^{60g}Co in the ground state and in the isomeric state ^{60m}Co. The decay schemes of cobalt from the ground ($T_{1/2}$=5.27 years) and isomer ($T_{1/2}$=10.47 minutes) states [9] are shown in Fig. 7. Isomer state has two decay modes – 99.76% isomeric gamma transition with $E_γ$=58.59 keV and 0.24% β$^-$ decay. The ground state is a well-known standard cobalt-source which after β$^-$ decay gives two

gamma lines 1333 keV and 1173 keV.

B. Indium sample

Natural indium consist of ^{113}In(4.29%) and ^{115}In(95.7%) isotopes [15]. After activation by neutrons in reaction (n,γ) isomer ^{116m}In is created which after β$^-$ decay with half-life 54.29 m transforms into ^{116}Sn in excited states with gamma lines $E\gamma$=417, 1097, 1293 and 2112 keV. The cross-section of reaction ^{115}In(n,γ) is near 200 barn [14].

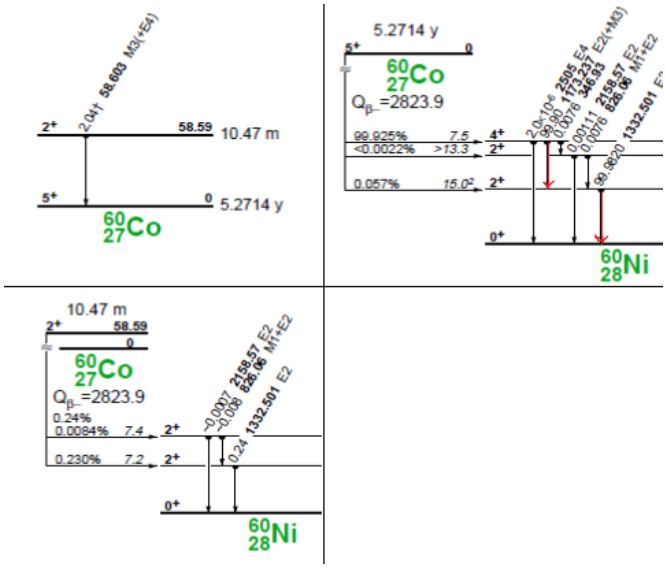

Fig. 8. The decay schemes of cobalt ground and isomer states [8].

VI. Results and Conclusions

A beryllium target and activation samples were irradiated for 10 minutes with a braking beam of gamma quanta obtained on a tungsten conversion target by an electron beam with an energy of 8.7 MeV and an intensity of 5 μA. Fig. 9 shows the gamma spectra from samples of indium, cobalt, and background. The isomeric cobalt line is not shown because it is located near channel 20 where the background is very high.

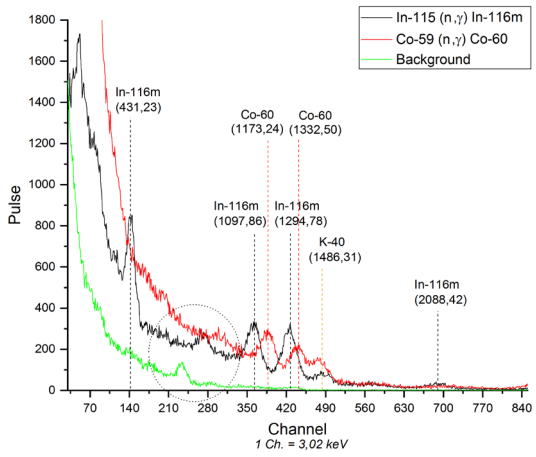

Fig. 9. The gamma spectra from activated ^{59}Co and ^{115}In samples and background spectrum.

The preliminary result of processing the gamma spectra of indium is given in [16], and the processing of cobalt spectra confirmed it, namely, at an electron beam current of 5 μA at an energy of 8.7 MeV and selected bremsstrahlung and neutron producing targets on the M-10 microtron we obtain a neutron flux 2×10^7 n/(cm^2·s).

The questions of neutron energy distribution and the ratio of neutron and gamma fields remain open [17,18].

Acknowledgment

This work was supported by the grant of the Ministry of Education and Science of Ukraine No. 0115U001098. V. Martishichkin thanks professor O.M. Parlag for a fruitful discussion about neutron detectors.

References

[1] V.I. Zhaba, I.I. Haysak, A.M. Parlag, V.S. Bokhinyuk, and M.M. Lazorka, "Energy dependence of cross section of photonuclear reactions on indium isotopes", *Problems of Atomic Science and Technology,* vol. 115, 2018, pp.155-158.
[2] A.A. Molnar, H.V. Vasylyeva, I.I. Haysak, M.T. Sabolchiy, I.M. Stoika, and A.A. Grabar, "Influence of the electron and gamma-irradiation on dielectric Properties of Sn2P2S6", *Uzh. Univ. Sci. Her. Ser. Phys.*, iss. 40, 2016, pp.13-17, 10.24144/2415-8038.2016.40.13-17
[3] M. Kralik, J. Solc, D. Chvatil, P. Krist, K. Turek, and C. Granja, "Microtron MT 25 as a source of neutrons*", Rev. Sci. Instrum., vol. 83, 083502*, Aug. 2012, 10.1063/1.4739404.
[4] D De Luca, L. Campajola, and P. Casolaro, "Neutron production with particle accelerators", *J. Phys.: Conf. Ser.,* vol. 1226, 012021, May 2019.
[5] A. P. Serebrov, M. E. Chaikovskii, G. N. Klyushnikov, O. M. Zherebtsov, and A. V. Chechkin, "Search for explanation of the neutron lifetime anomaly", *Phys. Rev. D 103, 074010*, Apr. 2021.
[6] C. Abel et al., "Measurement of the permanent electric dipole moment of the neutron", *Phys. Rev. Lett. 124, 081803*, Febr. 2020.
[7] M. D. Higgins, C. H. Greene, A. Kievsky, and M. Viviani, "Comprehensive study of the three- and four-neutron systems at low energies", *Phys. Rev. C **103**, 024004,* Febr. 2021.
[8] A. Nagornyi, V. I. Petrenko, M. Rajnak, I. V. Gapon, M. V. Avdeev, B. Dolnik, L. A. Bulavin, P. Kopcansky, M. Timko, "Particle assembling induced by non-homogeneous magnetic field at transformer oil-based ferrofluid/silicon crystal interface by neutron reflectometry", *Appl. Surf. Sci.*, vol. 473, 2019, pp. 912–917, 10.1016/j.apsusc.2018.12.197.
[9] R.B. Firestone, "Table of Isotopes". Eight edition // CD ROM Edition, Wiley-Interscience, 1996.
[10] A. Ferrari, P.R. Sala, J. Ranft, U. Siegen, "FLUKA: A multi-particle transport code". SLAC-R-773. (2015).
[11] I.I. Haysak, O.V. Takhtasyev, R.R. Holomb, K. Katovsky, A. Tanchak, J. Khushvaktov, A.A. Solnyshkin, "Monte Carlo simulation of bremsstrahlung spectra for low energy electron accelerators", in *2020 21st International Scientific Conference on Electric Power Engineering, EPE 2020*, Prague, Czech Republic, 2020, pp. 1-4, 10.1109/EPE51172.2020.9269252.
[12] V.P. Rudakov, "Passage of Ionizing Radiation Through Matter", in *Physical quantities: Handbook*, I. S. Grigoriev and E. Z. Meilikhova eds., Energoatomizdat, Moscow, 1991, p. 1170.
[13] "Handbook on photonuclear data for applications cross-sections and spectra", *IAEA*, Vienna, Austria, IAEA-TECDOC-1178, Oct. 2000.
[14] National Nuclear Data Center https://www.nndc.bnl.gov/sigma/
[15] J.K. Tuli, "Nuclear Wallet cards", *Brookhaven Nat. Lab.*, Upton, N-Y, USA, Jan. 2000.
[16] V. Martyshychkin *et al.*, "Generation of neutrons on Microtron M-10", in *2020 21st International Scientific Conference on Electric Power Engineering, EPE 2020*, Prague, Czech Republic, 2020, pp. 1-6, 10.1109/EPE51172.2020.9269218.
[17] X. Mao, K.R. Kase, and W.R. Nelson, "Giant dipole resonance neutron yields produced by electrons as a function of target material and thickness", *Health Phys.*, Feb. 1996, vol. 70, no. 2, p.207-214. 10.1097/00004032-199602000-00008.
[18] T.G. Soto-Bernal, A. Baltazar-Raigosa, D. Medina-Catro, and H.R. Vaga-Carrillo, "Neutron production during the interaction of monoenergetic electrons with tungsten foil in the radiotherapeutic energy range", *NIM Phys. Res. A*, vol. 868, Oct. 2017, P.27-38.